Available online at www.sciencedirect.com

ScienceDirect

Journal of the European Ceramic Society 29 (2009) 1687–1693

www.elsevier.com/locate/jeurceramsoc

Phase formation and characterization of high Curie temperature $x\mathrm{BiYbO_3}$–$(1-x)\mathrm{PbTiO_3}$ piezoelectric ceramics

Gao Feng*, Hong Rongzi, Liu Jiaji, Li Zhen, Cheng Lihong, Tian Changsheng

College of Material Science and Engineering, Northwestern Polytechnical University, Xi'an, 710072, China

Received 17 May 2008; received in revised form 26 August 2008; accepted 12 September 2008
Available online 12 November 2008

Abstract

Novel perovskite $x\mathrm{BiYbO_3}$–$(1-x)\mathrm{PbTiO_3}$ (BYPT) crystalline solutions were prepared by conventional ceramic processing. The effect of $BiYbO_3$ on the microstructure and electrical properties was investigated, and the reaction mechanism of phase formation was discussed. The results show that the proper calcining temperature is 860 °C and the optimum sintering temperature is 1140 °C. It is difficult for BYPT ceramics to obtain phase-pure perovskite structures. Pyrochlore phase $Yb_2Ti_2O_7$ was formed by Yb_2O_3 and TiO_2 that decomposed from $BiYbO_3$–$PbTiO_3$ at high temperature. With increasing $BiYbO_3$ content, the pyrochlore phase $Yb_2Ti_2O_7$ increases, which resulted in the decrease of densities and piezoelectric constants. The dielectric constants were in the range of 100–700 at room temperature and $\tan\delta$ less than 4%. BYPT ceramics with high Curie temperatures of >500 °C are obtained. $0.1\mathrm{BiYbO_3}$–$0.9\mathrm{PbTiO_3}$ ceramic is a very promising material for high-temperature (up to 550 °C) piezoelectric applications for high T_c, stable d_{33}, and high thermal-depoling temperature.

Keywords: Piezoelectric ceramics; Curie temperature; Pyrochlore phase; Electrical properties; $BiYbO_3$; $PbTiO_3$

1. Introduction

Piezoelectric sensors and actuators have experienced tremendous growth and wide spread application using $\mathrm{Pb(Zr,Ti)O_3}$ (PZT) materials.[1,2] Nowadays, both the automotive and aerospace industries have expressed the need for actuation and sensing at higher temperatures than currently available. Specifically, under-hood automotive applications such as internal vibration sensors, control surfaces, or active fuel injection nozzles require operation temperatures as high as 300 °C.[3,4] For example, active combustion control of spatial and temporal variations in the local fuel-to-air ratio is of considerable interest in lean gas turbine combustors. The actuator for fuel modulation in gas turbine combustors must meet requirement of operating temperature compatible with the fuel temperature, which is in the vicinity of 300 °C. However, PZT ceramics, with a maximum Curie temperature (T_c) of 385 °C, are generally limited to a maximum operating temperature of 190 °C.[5] It is 100 °C lower than the desired operating temperature for gas turbine combustor fuel-modulation injection valves. What is more, aerospace and aircraft industries use even higher standards, demanding systems to function at from 500 °C to 1000 °C. In view of these demands, it is necessary to develop high T_c piezoelectric materials.

Over the last few years an increasing amount of research has been done on the development of new piezoelectric materials with a high Curie temperature.[6–8] Eitel et al. state that a lower tolerance factor will result in a higher Curie temperature at the morphotropic phase boundary (MPB) and new high temperature ferroelectric materials based on $(1-x)\mathrm{BiScO_3}$–$x\mathrm{PbTiO_3}$ solid solutions with perovskite structure have been identified.[9–11] Guided by a perovskite tolerance factor relationship with T_c, low tolerance factor $BiMeO_3$ systems have projected transition temperatures greater than PZT; $BiMeO_3$–$PbTiO_3$ solid solutions such as $BiInO_3$–$PbTiO_3$,[12] $BiGaO_3$–$PbTiO_3$,[13] $BiFeO_3$–$PbTiO_3$[14,15] have been reported.

However, the potential applications of these systems are limited by the high cost of Sc_2O_3, In_2O_3 and Ga_2O_3 precursor oxides, and alternatives with a lower cost are desired. Moreover, the tolerance factor of $BiYbO_3$ is 0.857 that is lower than those of $BiScO_3$, $BiGaO_3$ and $BiInO_3$. Novel bismuth ytter-

---

* Corresponding author.
E-mail address: gaofeng@nwpu.edu.cn (G. Feng).

0955-2219/$ – see front matter © 2008 Elsevier Ltd. All rights reserved.
doi:10.1016/j.jeurceramsoc.2008.09.024

bium oxide-based ceramics have been investigated in this paper as a high Curie temperature piezoelectric. Lead titanate was used in solution with $BiYbO_3$ to help stabilize a perovskite $x$$BiYbO_3$–$(1-x)$$PbTiO_3$ (BYPT) phase. The phase structure and electrical properties of BYPT are investigated in detail.

2. Experimental

The general formula of the material studied was $x$$BiYbO_3$–$(1-x)$$PbTiO_3$ (designated as BYPT), where x is 0.05, 0.10, 0.15, and 0.20, respectively. Samples are numbered as $BYPT_1$, $BYPT_2$, $BYPT_3$, and $BYPT_4$ in sequence. Reagent pure Pb_3O_4, Bi_2O_3, TiO_2 and Yb_2O_3 were used as starting materials. The mixtures were weighed stoichiometrically and ball-milled for 12 h. The powders were calcined in air at 860 °C for 4 h. After milling for a second time, the powder was pressed into disks 12.0 mm in diameter at 100 MPa, and then sintered at 1100–1160 °C for 2 h under $PbO{\cdot}ZrO_2$ powder protection. The packing material $PbO{\cdot}ZrO_2$ was put on to a platinum sheet, and covered with an Al_2O_3 crucible to prevent PbO volatilization. The sintered discs were polished and pasted with silver on both surfaces. Samples were poled at 140 °C for 20 min under an electric field of 3 kV/mm in silicone oil. The piezoelectric properties were measured after 24 h aging at room temperature.

Differential scanning calorimetric and thermal gravimetric analysis (DSC and TGA, Model TA-SDT2960, American) studies were carried out from room temperature to 1200 °C at a heating rate of 10°/min. The content of the perovskite phase was examined by X-ray diffraction (XRD, Model Panalytical X'Pert PRO, Holland). For lead-based ferroelectrics, perovskite phase and pyrochlore phase always coexist. The relative amounts of perovskite and pyrochlore phases were determined by measuring the major X-ray peak intensities for perovskite and pyrochlore phases, i.e. (1 0 1) and (2 2 2), respectively. The percentage of perovskite phase was calculated by the following equation [16]:

$$\text{Content of perovskite phase}(\%) = \frac{I_{\text{perov}(1\,0\,1)}}{I_{\text{perov}(1\,0\,1)} + I_{\text{pyroc}(2\,2\,2)}} \times 100 \qquad (1)$$

where I_{perov} and I_{pyroc} stand for the intensities of the major peaks (1 0 1) and (2 2 2) for perovskite and pyrochlore phases, respectively. The microstructure was observed by scanning electron microscopy (SEM, Model Hitachi S-570, Japan). The temperature dependence of dielectric constant (ε) and dielectric loss ($\tan\delta$) were measured between 130 °C and 600 °C with a LCR precision electric bridge (Model HP4284, Hewlett-Packard). The piezoelectric constant (d_{33}) was measured with a quasistatic piezoelectric d_{33}-meter (Model ZJ-3D, Institute of Acoustics, Academic Sinica, China). Thermal-depoling experiments were executed by holding the poled samples for 2 h at various high temperatures, cooling to room temperature, measuring d_{33}, and repeating testing procedure up to 600 °C.

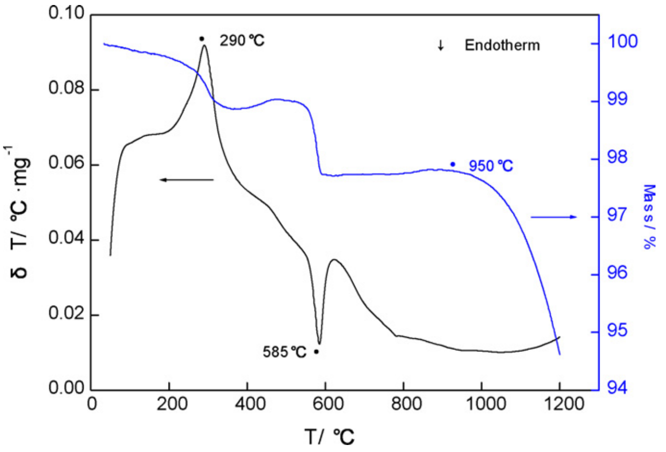

Fig. 1. DSC and TGA curves of $BYPT_2$ powders.

3. Results and discussion

Fig. 1 shows DSC and TGA curves of $BYPT_2$ powders. It is inferred from the DSC curve that an exothermic peak and a single endothermic peak are observed at temperatures of 290 °C

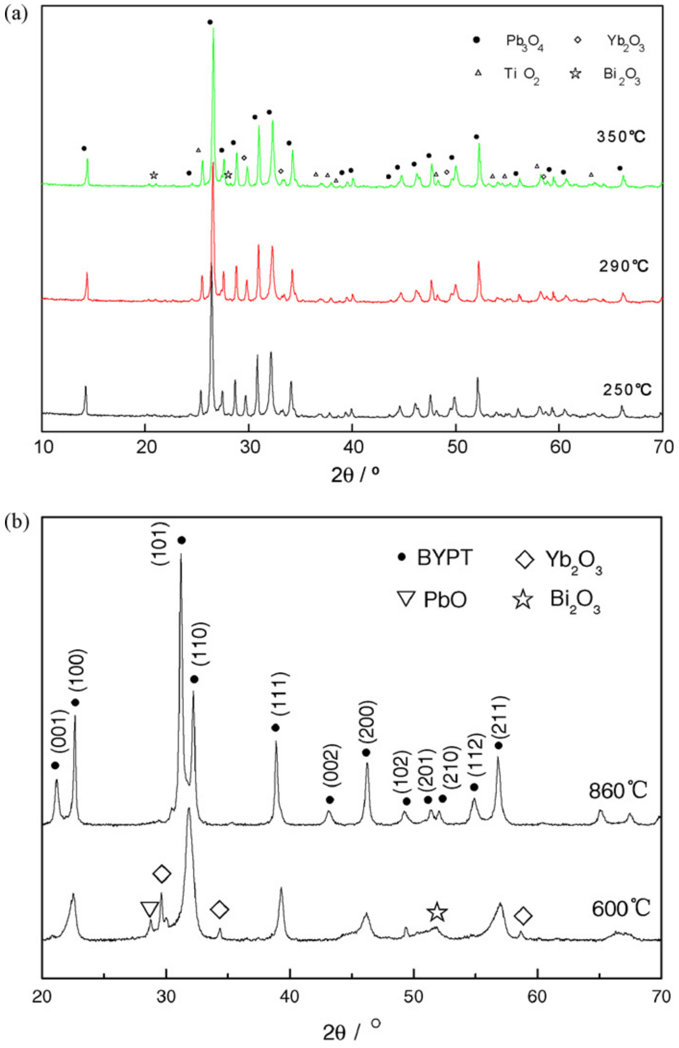

Fig. 2. The XRD patterns of $BYPT_2$ powders calcined at different temperatures.

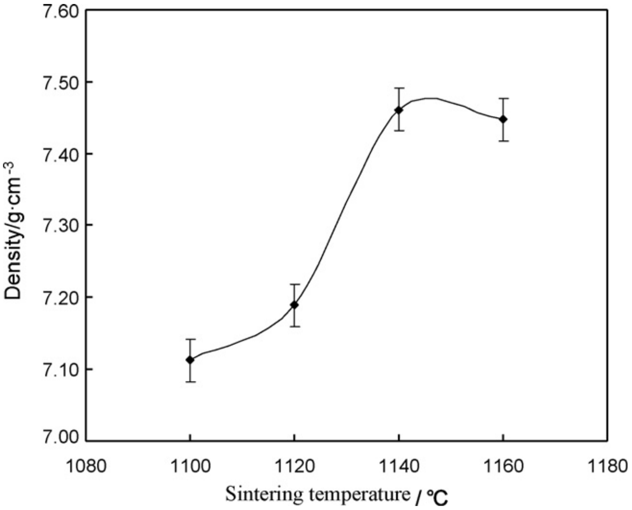

Fig. 3. Density of $BYPT_2$ ceramics sintered at different temperatures.

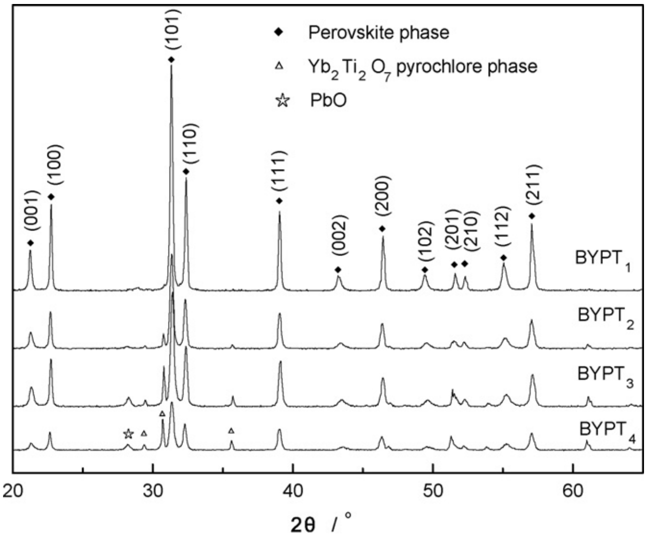

Fig. 4. The XRD patterns of BYPT ceramics sintered at 1140 °C.

and 585 °C, respectively. From TGA curve, it is found that percentage loss in the mass is more than 1% at 585 °C. When the temperature is higher than 950 °C, percentage loss in the mass increases largely because of the PbO evaporation.

In order to clarify the peaks in DSC curves, $BYPT_2$ powders were calcined at 250 °C, 290 °C and 350 °C. Fig. 2(a) shows XRD patterns of $BYPT_2$ powders. The peaks of original materials such as Pb_3O_4, Yb_2O_3, TiO_2 and Bi_2O_3 are observed and no other new phase is formed. There is no phase transition happened at 290 °C. The 290 °C peak in DSC curve should be attributed to some organic impurity decomposed at 290 °C. Fig. 2(b) shows XRD patterns of $BYPT_2$ powders calcined at 600 °C and 860 °C. The peaks of original materials such as PbO, Yb_2O_3, and Bi_2O_3 are observed and perovskite-typed BYPT is the main phase when $BYPT_2$ powders are calcined at 600 °C. After $BYPT_2$ powders are fired at 860 °C, it shows that the pure BYPY phase forms. The results mean that the endothermic peak at 585 °C is corresponding to the formation of the BYPT compound. And the proper calcining temperature for BYPT sample is 860 °C.

The densities of $BYPT_2$ ceramics sintered at different temperatures are shown in Fig. 3. It is found that the density increases quickly at temperature range from 1100 °C to 1140 °C. The maximum density, 7.46 g/cm^3, is achieved at 1140 °C. When the sintering temperature is higher than 1140 °C, the density decreases. The results indicate the optimum sintering temperature is 1140 °C.

Fig. 4 shows XRD patterns of BYPT ceramics sintered at 1140 °C. In general, in Pb-based ABO_3 materials, pyrochlore phase formation can be identified by a diffraction peak at $2\theta \sim 31°$. It is observed that the main phase is perovskite phase, and the others are $Yb_2Ti_2O_7$ pyrochlore phase and PbO phase. However, the instability of the perovskite phase in the low tolerance factor materials prevented the MPB compositions from being synthesized.

As listed in Table 1, the amounts of perovskite phase decrease with increasing content of $BiYbO_3$. It shows that the percentage of pyrochlore phase, $Yb_2Ti_2O_7$, amounts to 34.1% when x is 0.20. The tolerance factor for perovskites is given by the formula[5,9]:

$$t = \frac{r_A + r_O}{\sqrt{2}(r_B + r_O)} \quad (2)$$

where r_A and r_B are the ionic radius of the ions occupying the A, B positions, respectively, and r_O is the ionic radius of oxygen, and t is the Tolerance factor. It has been observed that a stable perovskite may be expected to form if $t = 0.88–1.09$, using Shannon's revised ionic radii. Ferroelectric perovskites with $t = 1$ may be expected to have a cubic symmetry, ferroelectric perovskites with $t < 1$ are usually rhombohedral or monoclinic while ferroelectric perovskites with $t > 1$ are commonly tetragonal. For $BiYbO_3$ compound, the relatively large ionic radius of Bi^{3+} (140 pm) in the A position and the small ionic radius of Yb^{3+} (86.8 pm)[17] in the B position, both referred to the general ABO_3 perovskite, result in a small tolerance factor 0.857. Perovskite with such tolerance factor is known to be difficult to synthesize and second phases often appear.

Based on the tolerance factor t, solid solutions of $BiScO_3$ ($t = 0.907$), $BiInO_3$ ($t = 0.884$) and $BiYbO_3$ ($t = 0.857$) with $PbTiO_3$ would exhibit morphotropic phase boundary (MPB) with the Curie temperature T_c's significantly greater than $Pb(Zr_{1-x}Ti_x)O_3$ and $PbTiO_3$ ($T_c = 490\,°C$) itself. For the $(1-x)BiScO_3–xPbTiO_3$ solid solution, a MPB was found at $x = 0.64$, with correspondingly enhanced dielectric and piezoelectric properties. For the system $(1-x)BiInO_3–xPbTiO_3$, phase pure perovskites could not be achieved even for $x \geq 0.9$.[9,10] The issue of perovskite stability was further com-

Table 1
Phase structure and sintered properties of BYPT ceramics.

Samples	$BYPT_1$	$BYPT_2$	$BYPT_3$	$BYPT_4$
Perovskite (%)	97.83	86.59	83.20	65.90
Pyrochlore (%)	2.17	13.41	16.80	34.10
Density (g/cm^3)	7.41	7.46	7.32	7.22
Relative density (%)	93.2	93.8	92.0	90.8
Average grain size (μm)	1.98	1.79	1.32	1.07

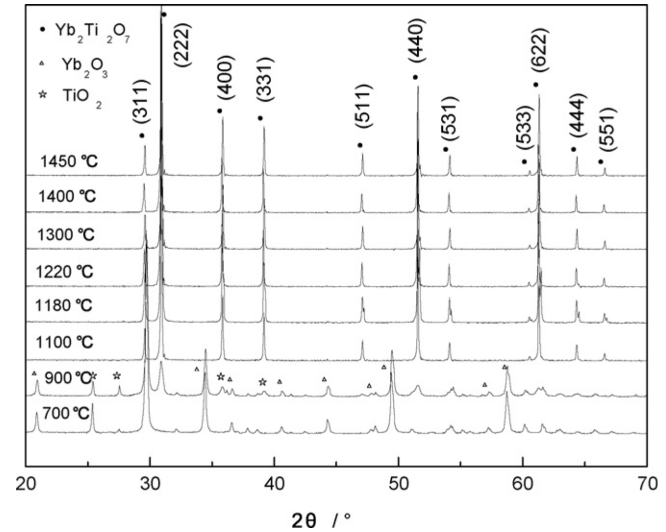

Fig. 5. The XRD patterns of $Yb_2Ti_2O_7$ sintered at different temperatures.

pounded for the $BiYbO_3$–$PbTiO_3$ system. Although $PbTiO_3$ is used to help stabilize a perovskite, the results demonstrate that it is difficult to synthesize pure perovskite phase for BYPT ceramics. So MPB composition of BYPT ceramics was not synthesized. Besides $Yb_2Ti_2O_7$ pyrochlore phase, PbO was also observed in $BYPT_3$ and $BYPT_4$ samples.

To investigate the reaction mechanism of BYPT ceramics and the stability of the $Yb_2Ti_2O_7$ phase, the $Yb_2Ti_2O_7$ pyrochlore compound is synthesized by sintering Yb_2O_3 and Bi_2O_3 at different temperatures. Fig. 5 shows XRD patterns of $Yb_2Ti_2O_7$ pyrochlore phase evolution with sintering temperatures. It is revealed that pure $Yb_2Ti_2O_7$ phase was not fabricated at 700 °C and 900 °C, but an increment of the sintering temperature to 1100 °C resulted in phase-pure $Yb_2Ti_2O_7$. It can be concluded that the synthesis temperature of $Yb_2Ti_2O_7$ is 900–1100 °C. And $Yb_2Ti_2O_7$ phase is stable though the sintering temperature increases to 1450 °C.

Thus the overall reaction of BYPT ceramics can be represented by the following equations:

$$\frac{x}{2}\mathrm{Bi_2O_3} + \frac{x}{2}\mathrm{Yb_2O_3} + (1-x)\mathrm{PbO} + (1-x)\mathrm{TiO_2} \xrightarrow{550\sim650\ ^\circ\mathrm{C}} x\mathrm{BiYbO_3}\text{–}(1-x)\mathrm{PbTiO_3} \tag{3}$$

It is well known that PbO has a low melting point (890 °C), it tends to evaporate at high sintering temperature, the equilibrium was destroyed and $PbTiO_3$ decomposes to TiO_2 and PbO, as shown in Eqs. (4) and (5):

$$\mathrm{PbO(s)} \overset{890\,^\circ\mathrm{C}}{\longleftrightarrow} \mathrm{PbO(g)} \overset{890\,^\circ\mathrm{C}}{\longleftrightarrow} \mathrm{Pb(g)} + \frac{1}{2}\mathrm{O_2(g)} \tag{4}$$

$$\mathrm{PbTiO_3} \xrightarrow{>890\,^\circ\mathrm{C}} \mathrm{TiO_2} + \mathrm{PbO} \tag{5}$$

What is more, because Bi_2O_3 has a low melting point (820 °C), unstable perovskite $BiYbO_3$ will decompose to Yb_2O_3 and Bi_2O_3. At last, the evaporation of PbO and Bi_2O_3 leads to exessive TiO_2 and Yb_2O_3, these two oxides are reacting at temperature higher than 900 °C and form stable $Yb_2Ti_2O_7$ pyrochlore phase, as shown in Eqs. (6)–(8):

$$\mathrm{Bi_2O_3(s)} \overset{820\,^\circ\mathrm{C}}{\longleftrightarrow} \mathrm{Bi_2O_3(g)} \overset{820\,^\circ\mathrm{C}}{\longleftrightarrow} 2\mathrm{Bi(g)} + \frac{3}{2}\mathrm{O_2(g)} \tag{6}$$

$$\mathrm{BiYbO_3} \xrightarrow{>820\,^\circ\mathrm{C}} \mathrm{Yb_2O_3} + \mathrm{Bi_2O_3} \tag{7}$$

$$2\mathrm{TiO_2} + \mathrm{Yb_2O_3} \xrightarrow{\geq 900\,^\circ\mathrm{C}} \mathrm{Yb_2Ti_2O_7} \tag{8}$$

$Yb_2Ti_2O_7$ has different grain shape comparing to the BYPT matrix grains. Fig. 6 shows the SEM photograph of $BYPT_2$ ceramics. The microstructure is composed of two types of grains. One type is irregularly shaped grains, the other is faceted rhombohedral grains. The elements content of two types of grains are determined by an energy-dispersive X-ray spectroscopy (EDS). The results are shown in Table 2. It is apparent that the rhombohedral grains are $Yb_2Ti_2O_7$ pyrochlore grains and the irregularly shaped grains are BYPT matrix grains with perovskite structure.

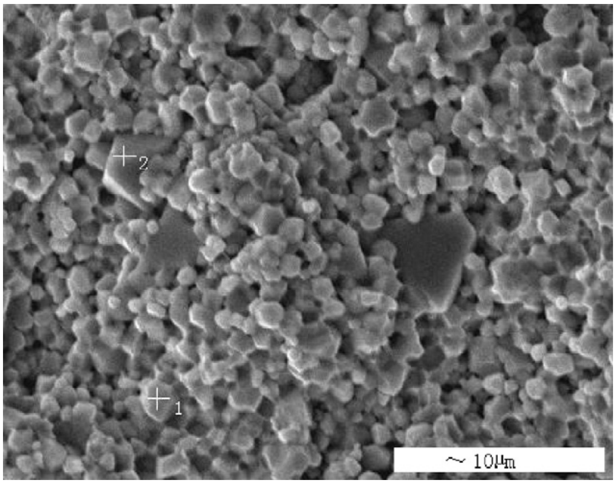

Fig. 6. Microstructure of $BYPT_2$ ceramic.

Fig. 7 shows the SEM photographs of BYPT ceramics sintered at 1140 °C. It can be seen that the sintered specimen is homogeneous and the fracture is intergranular. The microstructure of $BYPT_1$ and $BYPT_2$ are more uniform, the ceramics are sintered effectively with well-developed grain. An average grain size of ~2 μm is observed, as seen in Fig. 7(a) and (b), respectively. The average grain size decreases from 1.98 μm to 1.07 μm with increasing $BiYbO_3$. It seems that $BYPT_3$ and $BYPT_4$ sam-

Table 2
The element content of different grains in $BYPT_2$ ceramics.

Atomic (%)	O	Ti	Yb	Pb	Bi	Total
Spectrum 1	61.90	18.85	0.76	17.53	0.93	100.00
Spectrum 2	63.98	19.02	16.15	–	0.85	100.00

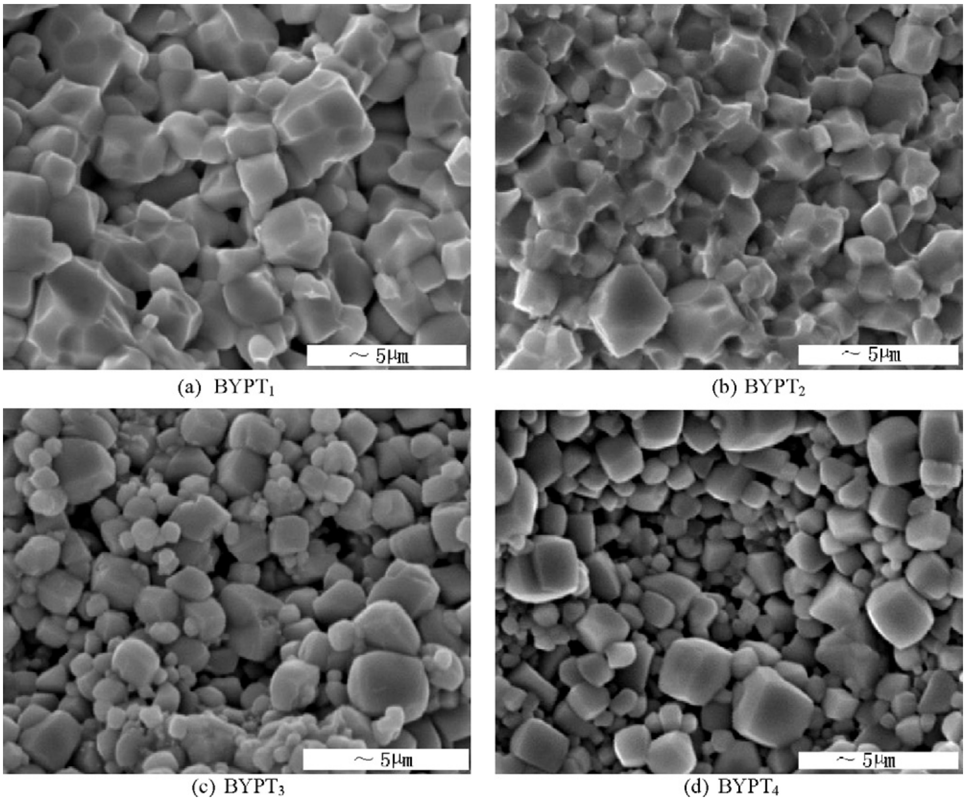

(a) $BYPT_1$ (b) $BYPT_2$

(c) $BYPT_3$ (d) $BYPT_4$

Fig. 7. The SEM photographs of BYPT ceramics sintered at 1140 °C.

ples are not dense, the grain boundaries are not clearly seen and some pores exist.

Fig. 8 shows the room temperature dielectric response as a function of $BiYbO_3$ content. The dielectric constant ε increases and then decreases with increasing $BiYbO_3$ content, while dielectric loss $\tan\delta$ shows the opposite trend. The dielectric constant ε varies in the range of 100–700, and the dielectric loss $\tan\delta$ is less than 4%. The BYPT ceramics with 0.10 mol $BiYbO_3$ has the optimum dielectric properties, ε is 660 and $\tan\delta$ is 0.017.

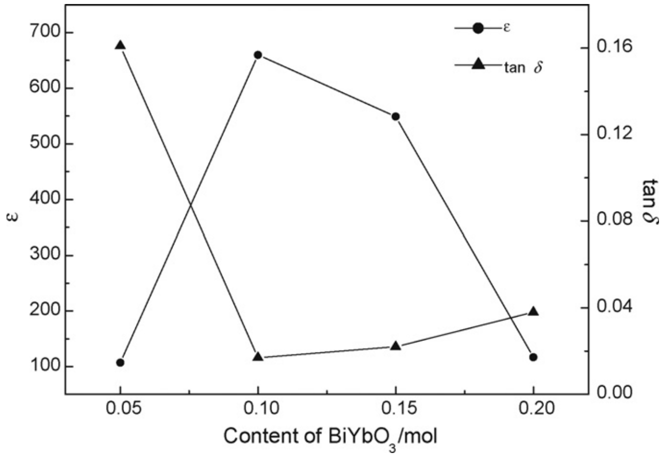

Fig. 8. The dielectric properties of BYPT ceramics at room temperature.

Fig. 9 shows the dielectric properties of BYPT ceramics as a function of temperature using a measurement frequency of 1 kHz. For $BYPT_1$ sample, the dielectric constant can be seen to slowly increase with increasing temperature from 130 °C to 500 °C. Then the dielectric constant subsequently increases as temperature rises higher than 500 °C, exhibiting a relatively sharp dielectric peak near 530 °C. This transition corresponds to the ferroelectric–paraelectric phase transformation at the Curie temperature. For higher $BiYbO_3$ contents ($x > 0.05$), the dielectric peaks are significantly wider, suggesting diffuse phase transition characteristic. It can be seen that the dielectric loss decreases from 500 °C to 540 °C, reaching a minimum, and increasing subsequently. The value of $\tan\delta$ is found to become very large at high temperatures, indicating space charge polarization and associated ionic conductivity.

Fig. 10 shows the variation of Curie temperature T_c and the piezoelectric constant d_{33} as a function of the content of $BiYbO_3$. It can be found that d_{33} decreases from 28 to 12 pC/N with increasing amount of $BiYbO_3$. For lead-based perovskite compounds, the pyrochlore phase can deteriorate dielectric and piezoelectric properties seriously. Because the amounts of $Yb_2Ti_2O_7$ pyrochlore phase increase with increasing content of $BiYbO_3$, this results in a decrease of d_{33}. As can be seen, the Curie temperature T_c increases firstly and then decreases with increasing amount of $BiYbO_3$. The optimized values for d_{33} of 18 pC/N and T_c of 590 °C are obtained for $BYPT_2$ ceramic.

In addition to measurements at room temperature, the piezoelectric activity was also studied as a function of temperature.

(a) Dielectric constant

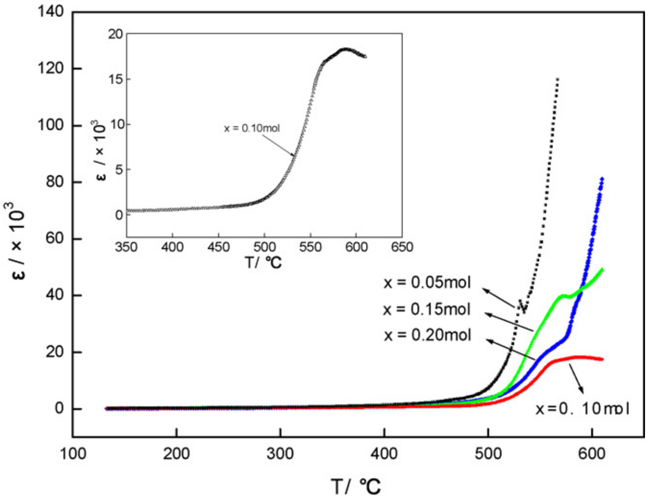

(b) Dielectric loss

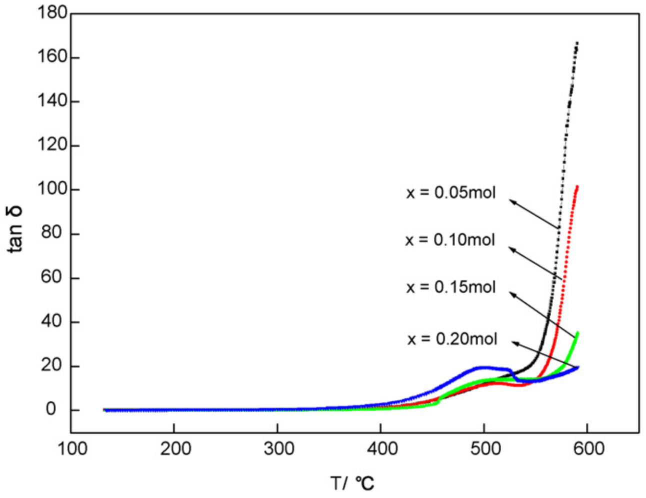

Fig. 9. The dielectric properties as a function of temperature for BYPT ceramics (1 kHz).

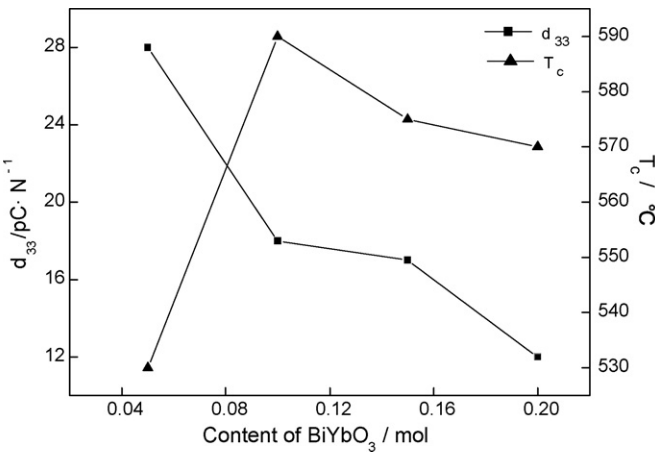

Fig. 10. The piezoelectric coefficient d_{33} and Curie temperature T_c of BYPT ceramics.

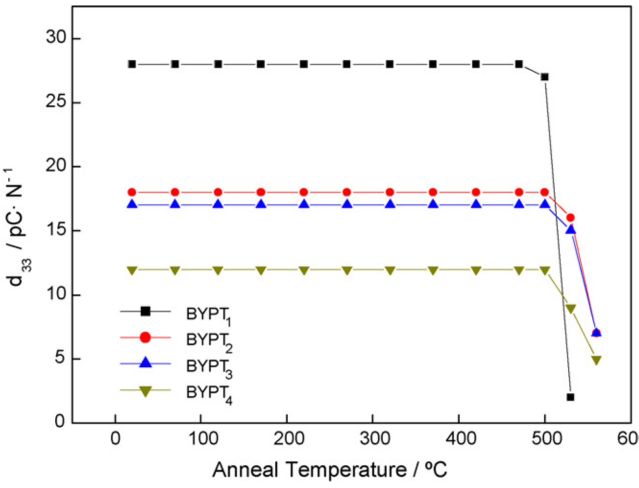

Fig. 11. Effect of annealing temperature on the piezoelectric coefficient d_{33} of BYPT ceramics.

The thermal-depoling behavior of the BYPT samples was shown in Fig. 11, in which piezoelectric constant d_{33} are plotted against the annealing temperature. The d_{33} of the BYPT$_1$ sample was stable up to 480 °C, and dropped rapidly above 500 °C, while the sample was fully depoled at 530 °C. The d_{33} values of the BYPT$_2$, BYPT$_3$, and BYPT$_4$ samples were stable up to 500 °C, above which these samples still maintained a significant piezoelectric activity at 550 °C with a relative decrease of coefficients smaller than 40%. They were fully depoled at temperatures between 570 °C and 600 °C.

It is worth noting that the BYPT$_2$ ceramics present piezoelectric coefficients significantly and can also maintain the piezoelectricity up to a temperature of 550 °C. Also, depoling occurs well below the Curie temperature at 590 °C, and so it could be possible to increase the temperature range of piezoelectric activity.

4. Conclusions

The microstructure and electrical properties of xBiYbO$_3$–$(1-x)$PbTiO$_3$ (BYPT) ceramics were investigated. The results show that the proper calcining temperature is 860 °C and the optimum sintering temperature is 1140 °C. It is difficult for BYPT ceramics to obtain phase-pure perovskite structures. There are perovskite and $Yb_2Ti_2O_7$ pyrochlore phases coexisting in the BYPT ceramics because of the evaporation of PbO and Bi_2O_3 at high temperature. With increasing BiYbO$_3$ content, the pyrochlore phase $Yb_2Ti_2O_7$ increases, which deteriorates the piezoelectric constant d_{33}. The dielectric constants at room temperature were in the range of 100–700 and dielectric loss less than 4%. The Curie temperature T_c increases firstly and then decreases with increasing BiYbO$_3$ content. Thermal-depoling studies demonstrated that d_{33} was stable up to 550 °C in 0.1BiYbO$_3$–0.9PbTiO$_3$. Therefore, a combination of high T_c, stable d_{33}, and high thermal-depoling temperature indicates that 0.1BiYbO$_3$–0.9PbTiO$_3$ is a very promising material for high-temperature (up to 550 °C) piezoelectric applications.

Acknowledgments

This work was supported by Natural Science Foundation of Shanxi Province in China, Science and Technology Innovation Fund of Northwestern Polytechnical University.

References

1. Hou, Y. D., Zhu, M. K., Wang, H., Wang, B., Yan, H. and Tian, C. S., Piezoelectric properties of new MnO_2-added 0.2PZN-0. 8PZT ceramics. *Mater. Lett.*, 2004, **58**, 1508–1512.
2. Takashi, H. and Tomoyuki, H., Piezoelectric properties of low-temperature sintered $Pb_{0.95}Ba_{0.05}[(Mg_{1/3}Nb_{2/3})_{0.125}Zr_{0.445}Ti_{0.43}]O_3$ ceramics with chemically-added $LiBiO_2$ sintering aid[J]. *J. Eur. Ceram. Soc.*, 2005, **25**, 2437–2441.
3. Chen, S., Dong, X., Mao, C. and Cao, F., Thermal stability of $(1-x)BiScO_3$–$xPbTiO_3$ piezoelectric ceramics for high-temperature sensor applications. *J. Am. Ceram. Soc.*, 2006, **89**(10), 3270–3272.
4. Sharma, S., Hall, D. A. and Mulage, P. S., Structural studies of $BiFeO_3$ modified BMZ-PT ceramics. *Mater. Lett.*, 2007, **61**, 3352–3356.
5. Snel, M. D., Groen, W. A. and With, G., New $Bi(Mg_{0.75}W_{0.25})O_3$–$PbTiO_3$ ferroelectric ceramics. *J. Eur. Ceram. Soc.*, 2006, **26**, 89–93.
6. Zhu, W. M. and Ye, Z. G., Ternary $Pb(Yb_{1/2}Nb_{1/2})O_3$–$PbZrO_3$–$PbTiO_3$ system as high-T_C/high-piezoelectric materials. *Ceram. Int.*, 2004, **30**, 1443–1448.
7. Zhang, S., Xia, R., Lebrun, L., Anderson, D. and Shrout, T. R., Piezoelectric materials for high power, high temperature applications. *Mater. Lett.*, 2005, **59**, 3471–3475.
8. Yan, H. X., Zhang, H., Ubic, R., Michael, J. R., Liu, J., Shen, Z. *et al.*, A lead-free high-Curie-point ferroelectric ceramic, $CaBi_2Nb_2O_9$. *Adv. Mater.*, 2005, **17**, 1261–1265.
9. Eitel, R. E., Randall, C. A., Shrout, T. R., Rehrig, P. W., Hackenberger, W. and Park, S. E., New high temperature morphotropic phase boundary piezoelectrics based on $Bi(Me)O_3$–$PbTiO_3$ ceramics. *Jpn. J. Appl. Phys.*, 2001, **40**, 5999–6002.
10. Eitel, R. E., Zhang, S. J., Shrout, T. R., Randall, C. A. and Levin, I., Phase diagram of the perovskite system $(1-x)$BiScO3–xPbTiO3. *J. Appl. Phys.*, 2004, **96**(5), 2828–2831.
11. Song, T. H., Eitel, R. E., Shrout, T. R., Randall, C. A. and Hackenberger, W., Piezoelectric properties in the perovskite $BiScO_3$–$PbTiO_3$–$(Ba, Sr)TiO_3$ ternary system. *Jpn. J. Appl. Phys.*, 2003, **42**, 5181–5184.
12. Duan, R., Speyer, R. F., Alberta, E. and Shrout, T. R., High Curie temperature perovskite $BiInO_3$–$xPbTiO_3$ ceramics. *J. Mater. Res.*, 2004, **19**(7), 2185–2192.
13. Cheng, J. R., Zhu, W., Li, N. and Cross, L. E., Fabrication and characterization of $xBiGaO_3$–$(1-x)PbTiO_3$: a high temperature reduced Pb-content piezoelectric ceramic. *Mater. Lett.*, 2003, **57**, 2090–2094.
14. Cheng, J. R., Li, N. and Cross, L. E., Structural and dielectric properties of Ga-modified $BiFeO_3$–$PbTiO_3$ crystalline solution. *J. Appl. Phys.*, 2003, **94**(8), 5153–5157.
15. Comyn, P., McBride, S. P. and Bell, A. J., Processing and electrical properties of $BiFeO_3$–$PbTiO_3$ ceramics. *Mater. Lett.*, 2004, **58**, 3844–3846.
16. Belsick, J. R., Halliyal, A., Kumar, U. and Newnham, R. E., Phase relations and dielectric properties of ceramics in the system $Pb(Zn_{1/3}Nb_{2/3})O_3$–$SrTiO_3$–$PbTiO_3$. *Am. Ceram. Soc. Bull.*, 1987, **66**(4), 664–667.
17. Yamashita, Y., Hosono, Y., Harada, K. and Ichinose, N., Effect of molecular mass of B-site ions on electromechanical coupling factors of lead-based perovskite piezoelectric materials. *Jpn. J. Appl. Phys.*, 2000, **39**, 5593–5596.